Pergamon

Int. J. Solids Structures Vol. 35, No. 23, pp. 3053–3069, 1998

0020-7683/98 $19.00 + .00

PII: S0020-7683(97)00355-7

COMPRESSIVE STIFFNESS OF ELASTIC LAYERS BONDED BETWEEN RIGID PLATES

HSIANG-CHUAN TSAI* and CHUNG-CHI LEE
Department of Construction Engineering, National Taiwan University of Science and Technology, P.O. Box 90-130, Taipei, Taiwan, R.O.C.

(*Received* 6 *March* 1997; *in revised form* 17 *November* 1997)

Abstract—The closed-form solutions to the compressive stiffness of elastic layers bonded between rigid plates are derived through theoretical analyses for the layers of infinite-strip, circular and square shapes. Based on the two kinematics assumptions, the governing equations for the mean pressure are established from the equilibrium equations and the bulk modulus equation. Satisfying the stress boundary conditions, the pressure functions are solved and the formulae for the compressive stiffness are derived. The compressive stiffnesses calculated from these formulae are extremely close to the results obtained from the finite element method for an extensive range of shape factor and Poisson's ratio. © 1998 Elsevier Science Ltd. All rights reserved.

1. INTRODUCTION

When an elastic layer is bonded between two rigid plates, the restricted lateral expansion on the bonded surfaces of the elastic layer causes a higher compression stiffness than the unbonded elastic layer in the direction normal to the layer. The effect becomes quite dramatic for an incompressible material. This mechanical characteristic has been adopted in the design of multilayered rubber bearings which are employed in many fields, e.g. thermal expansion bearings for highway bridges and isolation bearings to reduce buildings' seismic response.

By using approximate theoretical analyses, Gent and Lindley (1959) derived the compressive stiffness of incompressible elastic layers for infinite-strip shape and circular shape. Gent and Meinecke (1970) extended this analysis to the layers of square and other shapes. These approximate analyses are based on two kinematics assumptions and one stress assumption. They are (i) planes parallel to the rigid bounding plates remain plane and parallel; (ii) lines normal to the rigid bounding plates before deformation become parabolic after loading; (iii) the normal stress components in all three directions can be approximated by the mean pressure.

Although rubber can be treated as incompressible in some analyses, the assumption of incompressibility tends to overestimate the compressive stiffness of the bonded rubber layer when the layer's shape factor, defined as the ratio of the one bonded area to the force-free area, is high. Kelly (1993) developed a theoretical approach to derive the compressive stiffness considering the bulk compressibility's effect. Based on the above three assumptions, the relation between mean pressure and volume strain is reduced to a partial differential equation of the pressure, from which the compressive stiffnesses including the influence of volume change are derived. The solutions are available for the layers of infinite-strip shape (Chalhoub and Kely, 1991), circular shape (Chalhoub and Kelly, 1990) and square shape (Kelly, 1993). These solutions are accurate for the layers of high shape factor and the material of Poisson's ratio between 0.49 and 0.5, e.g. rubber, which is called an "approximate pressure" solution here.

In addition to the aforementioned two kinematic assumptions, Lindley (1979) postulated that the volume strain has a parabolic distribution across the layer's plane. He applied an energy method to derive the compressive stiffnesses of the infinite-strip and circular shapes which are accurate for the material of lower Poisson's ratios.

* Author to whom correspondence should be addressed.

Koh and Kelly (1989) utilized only the first two kinematic assumptions without the third stress assumption to derive the compressive stiffness for the square layer of compressible material by a "variable transform" approach. They also indicated that the parabolic deformation shape is indeed a realistic assumption.

In this paper, we derive the compressive stiffnesses of infinite-strip, circular and square shapes by theoretical analyses which are similar to the approach for the "approximate pressure" solution, but rely on the only two kinematic assumptions: horizontal planes remain plane and vertical lines become parabolic after loading. Partial differential equations of the pressure are initially derived from the equilibrium equations and the bulk modulus equation. Satisfying the stress boundary conditions of layers, the pressure functions are then solved, from which the compressive stiffnesses are derived. The derived compressive stiffnesses are compared with the results of finite element analysis to verify that the solutions are available for any value of Poisson's ratio.

2. GOVERNING EQUATIONS

Figure 1 indicates a layer of linearly elastic material is bonded between two rigid plates. The elastic layer is homogeneous and isotropic and has a thickness t and an area A. A rectangular Cartesian coordinate system (x, y, z) is established by locating the origin at the center of the layer and the x–y plane in the middle plane of the layer. Denote u, v and w be the displacements in the x, y and z coordinate directions, respectively. The layer's top and bottom surfaces are perfectly bonded to rigid plates so that $u = v = 0$ at $z = t/2$ and $z = -t/2$. Under direct compression in the z direction, the layer is deformed as shown in Fig. 2 and the displacements are assumed to have the form

$$u(x, y, z) = \bar{u}(x, y)\left(1 - \frac{4z^2}{t^2}\right) \tag{1}$$

$$v(x, y, z) = \bar{v}(x, y)\left(1 - \frac{4z^2}{t^2}\right) \tag{2}$$

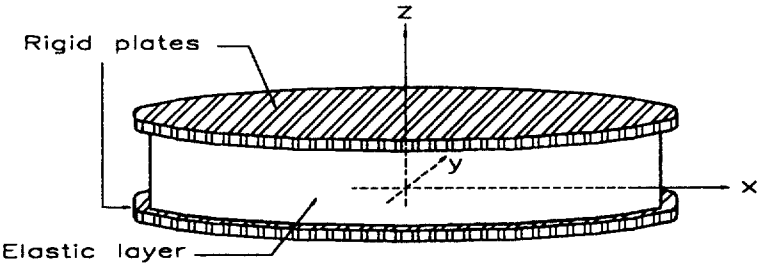

Fig. 1. Elastic layer bonded between rigid plates.

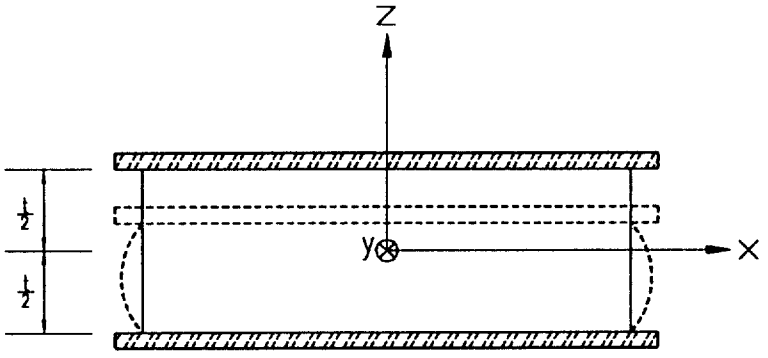

Fig. 2. Deformed shape of a compressed layer.

$$w(x, y, z) = \bar{w}(z) \tag{3}$$

Equations (1) and (2) satisfy the assumption that the vertical lines become parabolic; eqn (3) represents the assumption that horizontal planes remain plane.

For isotropic elastic material, the mean pressure p has the following relation with displacements

$$p(x, y, z) = -\kappa(u_{,x} + v_{,y} + w_{,x}) \tag{4}$$

where κ denotes the bulk modulus and the commas imply partial differentiation with respect to the indicated coordinate. Applying the following stress expressions

$$\sigma_{xx} = -\frac{\lambda}{\kappa}p + 2\mu u_{,x} \tag{5}$$

$$\sigma_{yy} = -\frac{\lambda}{\kappa}p + 2\mu v_{,y} \tag{6}$$

in which λ and μ represent Lame's constants, the equilibrium equations in the x and y coordinate directions become

$$u_{,xx} + u_{,yy} + u_{,zz} = \frac{\lambda + \mu}{\mu\kappa} p_{,x} \tag{7}$$

and

$$v_{,xx} + v_{,yy} + v_{,zz} = \frac{\lambda + \mu}{\mu\kappa} p_{,y} \tag{8}$$

Differentiating eqns (7) and (8) with respect to x and y, respectively, and adding them up yield

$$(u_{,x} + v_{,y})_{,xx} + (u_{,x} + v_{,y})_{,yy} + (u_{,x} + v_{,y})_{,zz} = \frac{\lambda + \mu}{\mu\kappa}(p_{,xx} + p_{,yy}) \tag{9}$$

Substituting the displacement assumptions in eqns (1) to (3) into eqn (4) and integrating the resulting equation through the thickness produce

$$\bar{u}_{,x} + \bar{v}_{,y} = \frac{3}{2}\left(\varepsilon_c - \frac{1}{\kappa}\bar{p}\right) \tag{10}$$

where $\bar{p}$ denotes the effective pressure defined as

$$\bar{p}(x, y) = \frac{1}{t}\int_{-t/2}^{t/2} p(x, y, z)\, dz \tag{11}$$

and ε_c represents the effective compression strain defined as

$$\varepsilon_c = -\frac{1}{t}\left[\bar{w}\left(\frac{t}{2}\right) - \bar{w}\left(-\frac{t}{2}\right)\right] \tag{12}$$

Similarly, after integrating through the layer's thickness, eqn (9) becomes

$$\frac{2}{3}[(\bar{u}_{,x}+\bar{v}_{,y})_{,xx}+(\bar{u}_{,x}+\bar{v}_{,y})_{,yy}]-\frac{8}{t^2}(\bar{u}_{,x}+\bar{v}_{,y})=\frac{\lambda+\mu}{\mu\kappa}(\bar{p}_{,xx}+\bar{p}_{,yy}) \tag{13}$$

The governing equation for the effective pressure is obtained by substituting eqn (10) into eqn (13),

$$\bar{p}_{,xx}+\bar{p}_{,yy}-2\alpha^2\bar{p}=-2\alpha^2\kappa\varepsilon_c \tag{14}$$

in which α is defined as

$$\alpha=\sqrt{\frac{6\mu}{t^2(\lambda+2\mu)}} \tag{15}$$

Equation (14) is solved by satisfying the boundary conditions that the stresses are free on the unbonded surface of the elastic layer. In the "approximate pressure" solution, the differential equation is similar to eqn (14), but the coefficient α is different; the boundary conditions are assumed as $\bar{p}(x, y) = 0$ on the stress-free surfaces.

The compressive stiffness of the layer is determined by the effective compression modulus defined as

$$E_c=\frac{-\int_A \bar{\sigma}_{zz}\,dx\,dy}{A\varepsilon_c} \tag{16}$$

In the above equation, the numerator represents the total applied compression force and $\bar{\sigma}_{zz}$ is the effective vertical stress defined as

$$\bar{\sigma}_{zz}=\frac{1}{t}\int_{-t/2}^{t/2}\sigma_{zz}\,dz \tag{17}$$

By using the following stress expression for the vertical stress,

$$\sigma_{zz}=-\frac{\lambda}{\kappa}p+2\mu w_{,z} \tag{18}$$

the effective compression modulus becomes

$$E_c=2\mu+\frac{\lambda}{A\kappa\varepsilon_c}\int_A \bar{p}\,dx\,dy \tag{19}$$

3. LAYER OF INFINITE-STRIP SHAPE

Figure 3 depicts an infinite-strip layer of width $2b$ and thickness t. If the y coordinate direction is attached to the infinite-long side, the displacement component v vanishes, so

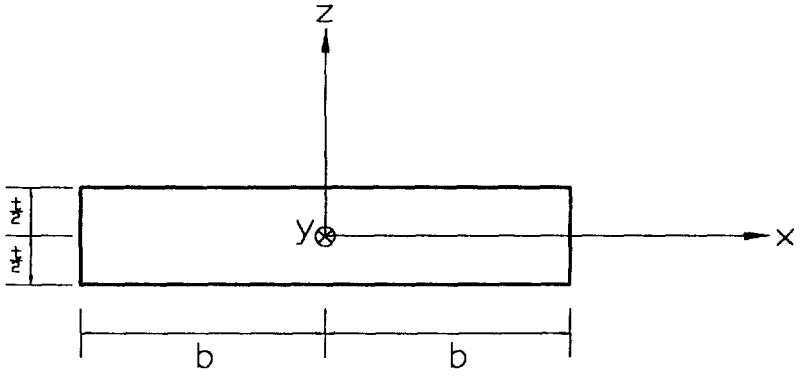

Fig. 3. Dimensions of an infinite-strip layer.

that the elastic layer is in plane strain state parallel to the xz plane. The governing equation for the effective pressure in eqn (14) becomes

$$\bar{p}_{,xx} - \bar{\alpha}^2 \bar{p} = -\bar{\alpha}^2 \kappa \varepsilon_c \tag{20}$$

in which

$$\bar{\alpha} = \sqrt{\frac{12\mu}{t^2(\lambda+2\mu)}} \tag{21}$$

Since $v_y = 0$, combining eqns (4) and (5) leads to

$$\sigma_{xx} = -\frac{\lambda+2\mu}{\kappa} p - 2\mu w_{,z} \tag{22}$$

By integrating the above equation through the thickness, the boundary condition $\sigma_{xx} = 0$ at $x = b$ yields

$$\bar{p}(b) = \frac{2\mu}{\lambda+2\mu} \kappa \varepsilon_c \tag{23}$$

By satisfying the above boundary condition, eqn (20) is solved as

$$\bar{p}(x) = \kappa \varepsilon_c \left[1 - \left(\frac{\lambda}{\lambda+2\mu} \right) \frac{\cosh(\bar{\alpha} x)}{\cosh(\bar{\alpha} b)} \right] \tag{24}$$

By substituting the above equation into eqn (19), the effective compression modulus for the infinite-strip layer is derived as

$$E_c = 2\mu + \lambda \left[1 - \left(\frac{\lambda}{\lambda+2\mu} \right) \frac{\tanh(\bar{\alpha} b)}{\bar{\alpha} b} \right] \tag{25}$$

The shape factor of the infinite-strip layer is defined as

$$S_i = \frac{b}{t} \tag{26}$$

According to eqn (21),

$$\bar{\alpha} b = 2 S_i \sqrt{\frac{3\mu}{\lambda+2\mu}} \tag{27}$$

Therefore, E_c defined in eqn (25) is a multiple of Young's modulus E and is a function of Poisson's ratio ν and shape factor S_i. The variations of E_c/E with ν for $S_i = 2$ and $S_i = 20$ are plotted in Fig. 4 and compared with the results computed by the finite element method. In the finite element solution, the infinite-strip layer is modeled by 8-node isoparametric plane-strain elements. According to this figure, the compressive modulus in eqn (25) is almost the same as the finite element solution.

The formula derived by Lindley (1979) for the compressive modulus of infinite-strip layer can be expressed as

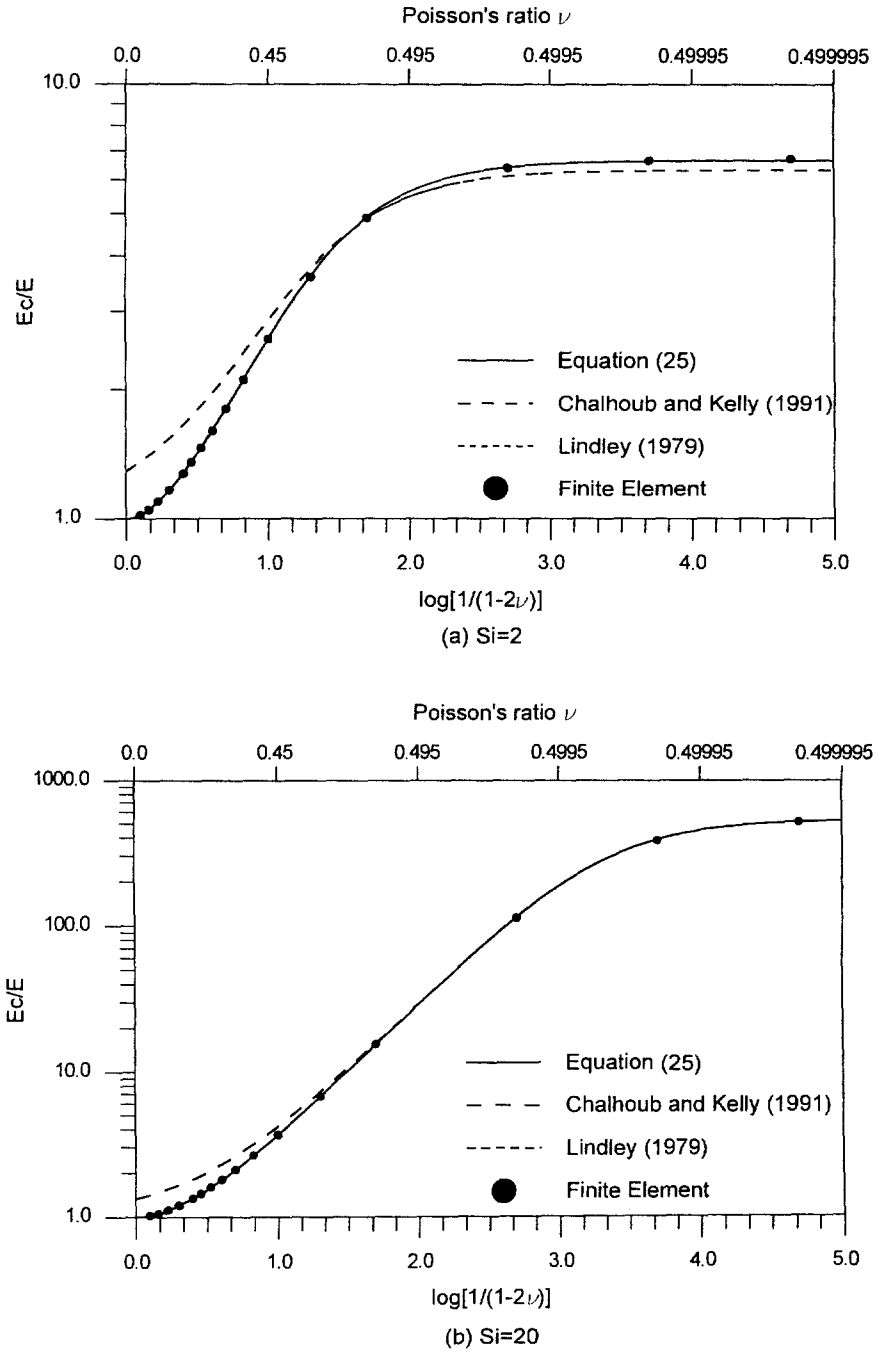

Fig. 4. Effective compression modulus of infinite-strip layer.

$$E_c = \begin{cases} 2\mu+\lambda\left[1-\left(\dfrac{\lambda}{\lambda+2\mu}\right)\left(1-\dfrac{1}{3}(\bar{\alpha}b)^2+\dfrac{\dfrac{2}{15}(\bar{\alpha}b)^4}{1+\dfrac{17}{42}(\bar{\alpha}b)^2}\right)\right] & \text{for} \quad \bar{\alpha}b < 3.24 \\ 2\mu+\lambda\left[1-\left(\dfrac{\lambda}{\lambda+2\mu}\right)\dfrac{0.972}{\bar{\alpha}b}\right] & \text{for} \quad \bar{\alpha}b \geqslant 3.24 \end{cases} \tag{28}$$

This formula is similar to eqn (25) except for the function $\bar{\alpha}b$. For smaller value of $\bar{\alpha}b$,

$$\frac{\tanh(\bar{\alpha}b)}{\bar{\alpha}b} \approx 1-\frac{1}{3}(\bar{\alpha}b)^2+\frac{2}{15}(\bar{\alpha}b)^4-\frac{17}{315}(\bar{\alpha}b)^6 \tag{29}$$

For larger value of $\bar{\alpha}b$, $\tanh(\bar{\alpha}b) \approx 1$. Therefore, eqn (28) is very close to eqn (25). This can be proved by the curves of the two equations plotted in Fig. 4. However, the expression in eqn (25) is more compact that eqn (28).

The "approximate pressure" solution derived by Chalhoub and Kelly (1991) is

$$E_c = 3\mu+\kappa\left[1-\frac{\tanh(\hat{\alpha}b)}{\hat{\alpha}b}\right] \tag{30}$$

with

$$\hat{\alpha}b = 2S_i\sqrt{\frac{3\mu}{\kappa}} \tag{31}$$

As shown in Fig. 4, the "approximate pressure" solution is accurate only in the case of high shape factor and near incompressibility.

In the layer's material is nearly incompressible, $\nu \approx 0.5$, the magnitude of λ becomes infinite and $\bar{\alpha}$ is infinitesimal. Substituting the following approximation

$$\frac{\tanh(\bar{\alpha}b)}{\bar{\alpha}b} \approx 1-\frac{1}{3}\bar{\alpha}^2b^2 = 1-4S_i^2\frac{\mu}{\lambda+2\mu} \tag{32}$$

into eqn (25) yields

$$E_c \approx \frac{4\mu(\lambda+\mu)}{\lambda+2\mu}+\frac{4\mu\lambda^2}{(\lambda+2\mu)^2}S_i^2 \tag{33}$$

The asymptotic solution of E_c for the infinite λ is

$$E_c = 4\mu(1+S_i^2) \tag{34}$$

which is the effective compression modulus for incompressible material and is the same as the result reported by Gent and Lindley (1959).

4. LAYER OF CIRCULAR SHAPE

The circular layer shown in Fig. 5 has a radius of b and a thickness of t. A cylindrical polar coordinate system (r, θ, z) is established with the origin at the center of the layer. The elastic layer is in the axisymmetric stress state so that the displacement in the θ direction vanishes. The displacement in the r direction, denoted as u, and the displacement in the z direction, denoted as w, are assumed as

$$u(r, z) = \bar{u}(r)\left(1 - \frac{4z^2}{t^2}\right) \tag{35}$$

$$w(r, z) = \bar{w}(z) \tag{36}$$

The mean pressure becomes

$$p(r, z) = -\kappa\left(u_{,r} + \frac{u}{r} + w_{,z}\right) \tag{37}$$

By applying the following stress expressions,

$$\sigma_{rr} = -\frac{\lambda}{\kappa}p + 2\mu u_{,r} \tag{38}$$

$$\sigma_{\theta\theta} = -\frac{\lambda}{\kappa}p + 2\mu\frac{u}{r} \tag{39}$$

the equilibrium equation in the r direction becomes

$$u_{,zz} - w_{,rz} = \frac{\lambda + 2\mu}{\mu\kappa}p_{,r} \tag{40}$$

Substituting the displacement assumptions in eqns (35) and (36) into eqns (37) and (40) and integrating the resulting equations through the thickness leads to

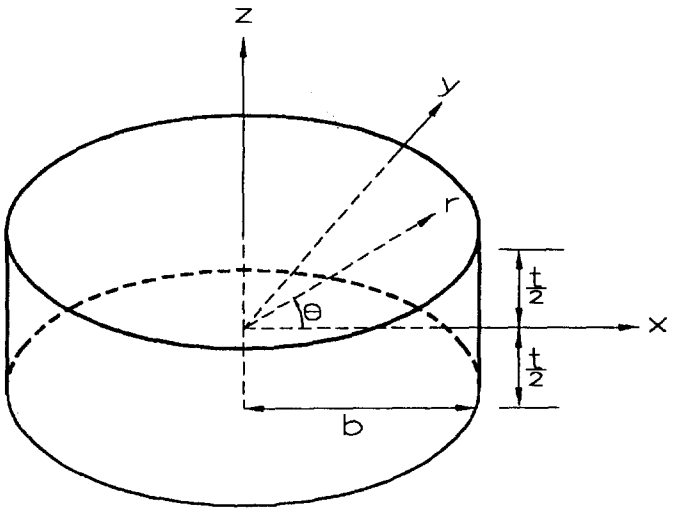

Fig. 5. Dimensions of a circular layer.

$$\bar{u}_{,r}+\frac{\bar{u}}{r}=\frac{3}{2}\varepsilon_c-\frac{3}{2\kappa}\bar{p} \tag{41}$$

and

$$\bar{u}=-\frac{t^2}{8}\frac{\lambda+2\mu}{\mu\kappa}\bar{p}_{,r} \tag{42}$$

The governing equation for the effective pressure, which may be derived by combining eqns (41) and (42) or taking coordinate transformation from eqn (14), is

$$\bar{p}_{,rr}+\frac{1}{r}\bar{p}_{,r}-\bar{\alpha}^2\bar{p}=-\bar{\alpha}^2\kappa\varepsilon_c \tag{43}$$

where $\bar{\alpha}$ is defined in eqn (21).

By substituting eqn (35) into eqn (38) and integrating the resulting equation through the thickness, the boundary condition $\sigma_{rr}=0$ at $r=b$ yields

$$\bar{p}(b)=\frac{4\mu\kappa}{3\lambda}\bar{u}_{,r}(b) \tag{44}$$

By combining the above equation with eqns (41) and (42), the boundary condition for the effective pressure becomes

$$\frac{1}{b}\bar{p}_{,r}(b)-\frac{6}{t^2}\bar{p}(b)+\bar{\alpha}^2\kappa\varepsilon_c=0 \tag{45}$$

By satisfying the above boundary condition, eqn (43) is solved as

$$\bar{p}(r)=\kappa\varepsilon_c\left[1-\frac{\bar{\alpha}b\left(1-\frac{1}{6}(\bar{\alpha}t)^2\right)}{\bar{\alpha}bI_0(\bar{\alpha}b)-\frac{1}{6}(\bar{\alpha}t)^2I_1(\bar{\alpha}b)}I_0(\bar{\alpha}r)\right] \tag{46}$$

where I_0 and I_1 denote the modified Bessel functions of the first kind of order 0 and order 1, respectively. The effective compression modulus for the circular layer is obtained by substituting eqn (46) into eqn (19)

$$E_c=\lambda+2\mu-\frac{\lambda^2}{(\lambda+2\mu)\frac{\bar{\alpha}bI_0(\bar{\alpha}b)}{2I_1(\bar{\alpha}b)}-\mu} \tag{47}$$

The shape factor of the circular layer is

$$S_c=\frac{b}{2t} \tag{48}$$

Therefore,

$$\bar{\alpha}b = 4S_c\sqrt{\frac{3\mu}{\lambda+2\mu}} \tag{49}$$

Figure 6 plots the effective compression modulus calculated by eqn (47) and the formulae published previously with respect to ν for $S_c = 2$ and $S_c = 20$. Also plotted in the figure is the finite element solutions where the circular layer is modeled by 8-node isoparametric elements of axisymmetry. The figure depicts that the compressive modulus calculated by eqn (47), the finite element method and the formula of Lindley (1979) are nearly the same

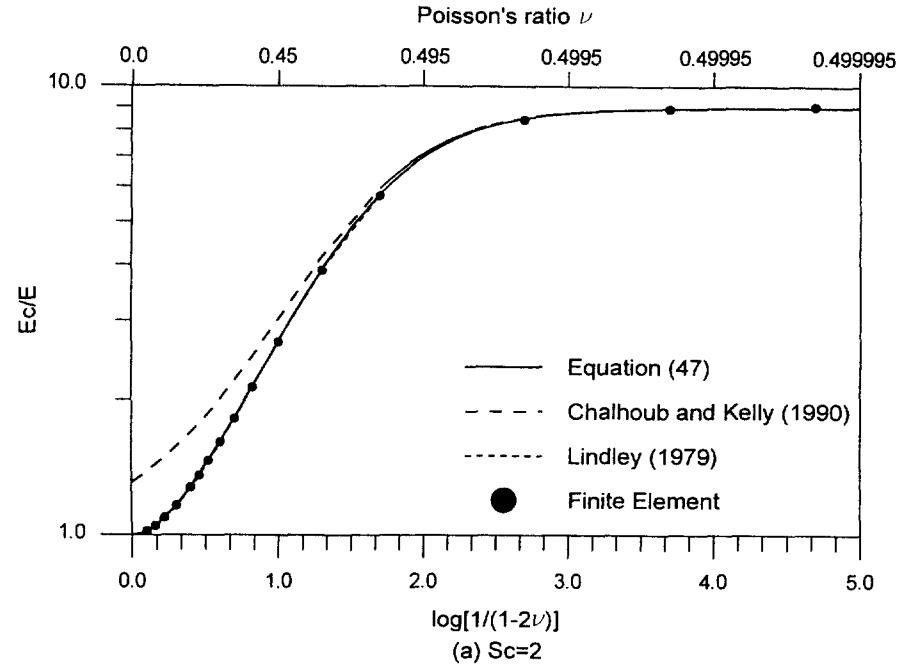

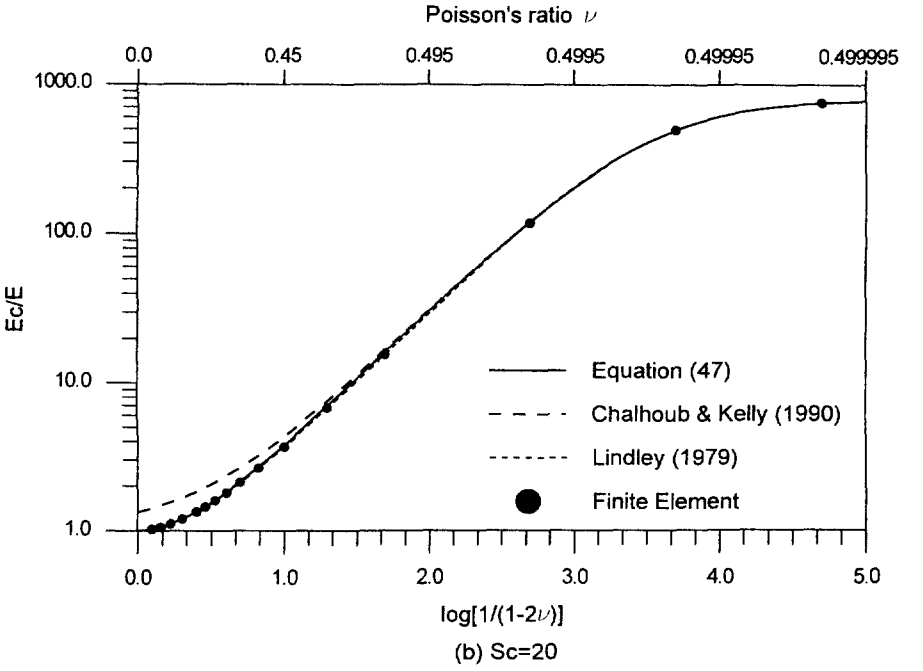

Fig. 6. Effective compression modulus of circular layer.

for any value of Poisson's ratio; the "approximate pressure" solution (Chalhoub and Kelly, 1990) loses accuracy when $\nu < 0.45$.

When the layer's material is nearly incompressible, $\bar{\alpha}b$ tends to infinitesimal and the following function of $\bar{\alpha}b$ in eqn (47) may be approximated by

$$\frac{\bar{\alpha}bI_0(\bar{\alpha}b)}{2I_1(\bar{\alpha}b)} \approx 1+\frac{1}{8}(\bar{\alpha}b)^2 = 1+6S_c^2\frac{\mu}{\lambda+2\mu} \tag{50}$$

Consequently, the effective compression modulus for incompressible material becomes

$$E_c = 3\mu(1+2S_c^2) \tag{51}$$

which is the same as the results reported by Gent and Lindley (1959).

5. LAYER OF SQUARE SHAPE

The square layer depicted in Fig. 7 has a side length of $2b$ and a thickness of t. Because of the square layer's symmetry around the x axis, the y axis and the diagonals of the square, the effective pressure has the following properties

$$\bar{p}(x,y) = \bar{p}(-x,y) = \bar{p}(x,-y) \tag{52}$$

and

$$\bar{p}(x,y) = \bar{p}(y,x) \tag{53}$$

The horizontal displacements possess the relation

$$\bar{u}(x,y) = \bar{v}(y,z) \tag{54}$$

which implies

$$\bar{u}_{,x}(x,y) = \bar{v}_{,y}(y,x) \tag{55}$$

Substituting eqns (1) and (2) into eqns (5) and (6), respectively, and integrating the resulting equations through the thickness, the boundary condition $\sigma_{xx} = 0$ at $x = b$ yields

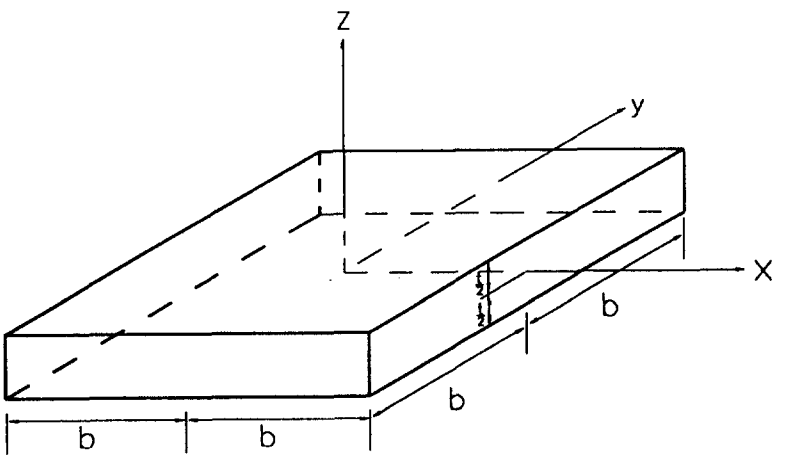

Fig. 7. Dimensions of a square layer.

$$\bar{p}(b,y) = \frac{4\mu\kappa}{3\lambda}\bar{u}_{,x}(b,y) \tag{56}$$

and $\sigma_{yy} = 0$ at $y = b$ provides

$$\bar{p}(x,b) = \frac{4\mu\kappa}{3\lambda}\bar{v}_{,y}(x,b) \tag{57}$$

Similarly, $\tau_{xy} = 0$ at $x = b$ gives

$$\bar{u}_{,y}(b,y) + \bar{v}_{,x}(b,y) = 0 \tag{58}$$

By combining eqns (10), (56) and (57), the effective pressure on the corner is found as

$$\bar{p}(b,b) = \frac{\mu\kappa}{\lambda+\mu}\varepsilon_c \tag{59}$$

According to the governing equation in eqn (14), the particular solution for $\bar{p}$ is

$$\bar{p}_p = \kappa\varepsilon_c \tag{60}$$

The complementary solution, denoted as $\bar{p}_c$, is solved by the method of separation of variables. By setting $\bar{p}_c(x,y) = \bar{X}(x)\bar{Y}(y)$, the functions $\bar{X}$ and $\bar{Y}$ are derived from the following equation

$$\frac{\bar{X}'' - \alpha^2\bar{X}}{\bar{X}} = -\frac{\bar{Y}'' - \alpha^2\bar{Y}}{\bar{Y}} = C \tag{61}$$

where C represents a constant. Denote $\bar{p}_0$, $\bar{p}_+$ and $\bar{p}_-$ are the solutions of $\bar{p}_c$ when $C = 0$, $C > 0$ and $C < 0$, respectively. The complete solution for $\bar{p}$ becomes

$$\bar{p}(x,y) = \bar{p}_p(x,y) + \bar{p}_0(x,y) + \bar{p}_+(x,y) + \bar{p}_-(x,y) \tag{62}$$

The following conditions are set on the corners

$$\bar{p}_+(b,b) = \bar{p}_-(b,b) = 0 \tag{63}$$

which implies, based on eqns (59) and (60), that

$$\bar{p}_0(b,b) = -\frac{\lambda\kappa}{\lambda+\mu}\varepsilon_c \tag{64}$$

The function $\bar{p}_0(x,y)$ is solved by satisfying the conditions in eqns (52) and (64)

$$\bar{p}_0(x,y) = -\frac{\lambda\kappa}{\lambda+\mu}\varepsilon_c\frac{\cosh(\alpha x)\cosh(\alpha y)}{\cosh^2(\alpha b)} \tag{65}$$

To satisfy eqns (52) and (63), $\bar{p}_+$ and $\bar{p}_-$ have the expressions

$$\bar{p}_+(x,y) = \sum_{n=1}^{\infty} A_n \cosh(\beta_n x)\cos(\gamma_n y) \tag{66}$$

$$\bar{p}_-(x,y) = \sum_{n=1}^{\infty} B_n \cos(\gamma_n x)\cosh(\beta_n y) \tag{67}$$

with

$$\gamma_n = \frac{(2n-1)\pi}{2b} \quad n = 1,2,\ldots,\infty \tag{68}$$

and

$$\beta_n = \sqrt{2\alpha^2+\gamma_n^2} \tag{69}$$

where A_n and B_n are the constants to be determined. The condition in eqn (53) gives $A_n = B_n$. Therefore, the effective pressure has the following expression

$$\bar{p}(x,y) = \kappa\varepsilon_c\left[1-\frac{\lambda}{\lambda+\mu}\frac{\cosh(\alpha x)\cosh(\alpha y)}{\cosh^2(\alpha b)}\right] + \sum_{n=1}^{\infty} A_n[\cosh(\beta_n x)\cos(\gamma_n y)+\cos(\gamma_n x)\cosh(\beta_n y)] \tag{70}$$

By substituting the above equation into eqn (19), the effective compression modulus becomes

$$E_c = \lambda+2\mu-\frac{\lambda^2}{\lambda+\mu}\frac{\tanh^2(\alpha b)}{(\alpha b)^2}+2\sum_{n=1}^{\infty} a_n \tag{71}$$

with

$$a_n = \frac{\lambda}{\varepsilon_c\kappa}A_n\frac{\sinh(\beta_n b)\sin(\gamma_n b)}{(\beta_n b)(\gamma_n b)} \tag{72}$$

To find A_n or a_n, substitute the expression of $\bar{p}(b,y)$ obtained from eqn (70) into eqn (56) to obtain $\bar{u}_{,x}(b,y)$. Then, applying eqn (55) yields

$$\bar{v}_{,y}(y,b) = \frac{3\lambda}{4\mu}\varepsilon_c\left[1-\frac{\cosh(\alpha y)}{\cosh(\alpha b)}\right]+\frac{3\lambda}{4(\lambda+\mu)}\varepsilon_c\frac{\cosh(\alpha y)}{\cosh(\alpha b)}+\frac{3\lambda}{4\mu\kappa}\sum_{n=1}^{\infty} A_n\cosh(\beta_n b)\cos(\gamma_n y) \tag{73}$$

In addition, substituting the expressions of $\bar{p}(b,y)$ and $\bar{u}_{,x}(b,y)$ into eqn (10) leads to

$$\bar{v}_{,y}(b,y) = \frac{3\lambda}{4\mu}\varepsilon_c\left[\frac{\cosh(\alpha y)}{\cosh(\alpha b)}-1\right]+\frac{3\lambda}{4(\lambda+\mu)}\varepsilon_c\frac{\cosh(\alpha y)}{\cosh(\alpha b)} - \left(\frac{3}{2\kappa}+\frac{3\lambda}{4\mu\kappa}\right)\sum_{n=1}^{\infty} A_n\cosh(\beta_n b)\cos(\gamma_n y) \tag{74}$$

Equations (73) and (74) indicate

$$\bar{v}_{,y}(x,y) = \frac{3\lambda}{4\mu}\varepsilon_c\left[-\frac{\cosh(\alpha x)}{\cosh(\alpha b)}+\frac{\cosh(\alpha y)}{\cosh(\alpha b)}\right]+\frac{3\lambda}{4(\lambda+\mu)}\varepsilon_c\frac{\cosh(\alpha x)\cosh(\alpha y)}{\cosh^2(\alpha b)}$$
$$+\sum_{n=1}^{\infty}A_n\left[\frac{3\lambda}{4\mu\kappa}\cos(\gamma_n x)\cosh(\beta_n y)-\left(\frac{3}{2\kappa}+\frac{3\lambda}{4\mu\kappa}\right)\cosh(\beta_n x)\cos(\gamma_n y)\right] \quad (75)$$

The expressions for $\bar{u}(x,y)$ and $\bar{v}(x,y)$ can be derived by integrating the above equation and satisfying the condition $\bar{v}(0,0)=0$ and the symmetric relation in eqn (54). The derived expressions of $\bar{u}(x,y)$ and $\bar{v}(x,y)$ must satisfy the condition in eqn (58), thereby yielding

$$\sum_{n=1}^{\infty}A_n\left[\frac{\lambda}{\mu\kappa}\left(\frac{\gamma_n}{\beta_n}+\frac{\beta_n}{\gamma_n}\right)+\frac{2}{\kappa}\frac{\beta_n}{\gamma_n}\right]\left[\frac{\sinh(\beta_n y)}{\sinh(\beta_n b)}+\frac{\sin(\gamma_n y)}{\sin(\gamma_n b)}\right]\sinh(\beta_n b)\sin(\gamma_n b)$$
$$=\varepsilon_c\left[\left(\frac{2\lambda}{\lambda+\mu}\tanh(\alpha b)-\frac{\lambda}{\mu}\alpha b\right)\frac{\sinh(\alpha y)}{\cosh(\alpha b)}-\frac{\lambda}{\mu}(\alpha y)\tanh(\alpha b)\right] \quad (76)$$

Multiplying the both sides of eqns (76) by $\sin(\gamma_m y)$ and taking the integration from $y=-b$ to $y=b$ produce

$$\sum_{n=1}^{\infty}D_{mn}a_n = d_m \quad m=1,2,\ldots,\infty \quad (77)$$

in which

$$D_{mn}=\left\{\delta_{mn}+\frac{2\beta_n b}{[(\gamma_m b)^2+(\beta_n b)^2]\tanh(\beta_N b)}\right\}\left[(\gamma_n b)^2+\left(1+2\frac{\mu}{\lambda}\right)(\beta_n b)^2\right] \quad (78)$$

with

$$\delta_{mn}=\begin{cases}1, & m=n\\ 0, & m\neq n\end{cases} \quad (79)$$

and

$$d_m = 2\lambda\left(\frac{\alpha b}{\gamma_m b}\right)^2\left[\frac{2\mu}{\lambda+\mu}\frac{\tanh(\alpha b)}{\alpha b}\frac{1}{1+\left(\frac{\alpha b}{\gamma_m b}\right)^2}-\frac{\tanh(\alpha b)}{\alpha b}-\frac{1}{1+\left(\frac{\alpha b}{\gamma_m b}\right)^2}\right] \quad (80)$$

In eqn (77), if a finite upper bound of m and n, say k, replaces the infinity, eqn (77) can be replaced by a matrix form

$$\mathbf{Da}=\mathbf{d} \quad (81)$$

where $\mathbf{D}$ denotes a $k\times k$ matrix formed by the elements D_{mn}; $\mathbf{a}$ and $\mathbf{d}$ are the k-dimensional vectors formed by the components a_n and d_m, respectively. Approximated values of a_n can be solved from eqn (81).

The shape factor of the bonded square layer is defined as

$$S_s=\frac{b}{2t} \quad (82)$$

According to eqn (15),

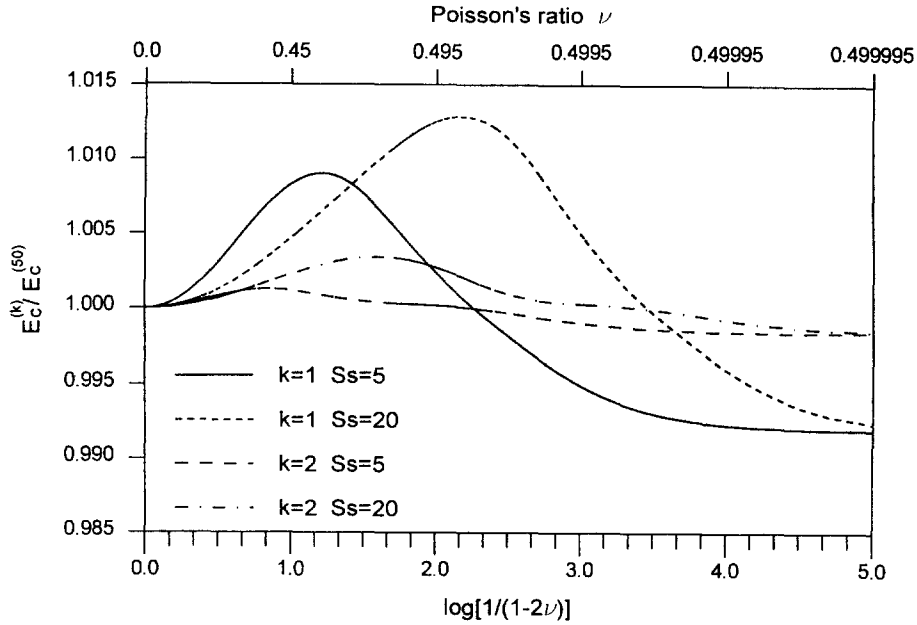

Fig. 8. Convergence of solution to the compression modulus of square layer.

$$\alpha b = 2S_s\sqrt{\frac{6\mu}{\lambda+2\mu}} \tag{83}$$

Let $E_c^{(k)}$ denote the value of E_c in eqn (71), including the first k terms of a_n. The ratio of $E_c^{(k)}/E$ is a function of ν and S_s. Figure 8 plots the ratios of $E_c^{(1)}/E_c^{(50)}$ and $E_c^{(2)}/E_c^{(50)}$ for the varied ν and two different S_s values. This figure reveals that the difference ratio between $E_c^{(1)}$ and $E_c^{(50)}$ is smaller than 0.015, which indicates that we can employ only the first term of a_n to obtain an extremely good approximation of E_c. The explicit form of $E_c^{(1)}$ is derived from eqns (81) and (71)

$$E_c^{(1)} = 2\mu+\lambda\left[1-\frac{1}{1+\dfrac{\mu}{\lambda}}\frac{\tanh^2(\alpha b)}{(\alpha b)^2}\right] - \frac{2\lambda(\alpha b)^2\left\{1+\dfrac{\tanh(\alpha b)}{\alpha b}\left[1-\dfrac{2\mu}{\lambda+\mu}+\dfrac{4}{\pi^2}(\alpha b)^2\right]\right\}}{\left[\dfrac{\pi^2}{4}+(\alpha b)^2+\dfrac{\beta_1 b}{\tanh(\beta_1 b)}\right]\left[\left(1+\dfrac{\mu}{\lambda}\right)\dfrac{\pi^2}{4}+\left(1+2\dfrac{\mu}{\lambda}\right)(\alpha b)^2\right]} \tag{84}$$

The values of the effective compression modulus calculated from eqn (84) are compared with the results computed by the finite element method in Fig. 9. In the finite element analysis, the square layer is modeled by 8-node solid elements with incompatible bending modes. The figure shows that the compressive modulus in eqn (84) is extremely close to the finite element solutions for any value of Poisson's ratio. The figure also plots the curves calculated by the methods published before, indicating that the "approximate pressure" solution (Kelly, 1993) loses accuracy when $\nu < 0.45$.

When the layer's material is nearly incompressible, the magnitude of λ becomes infinite and α is infinitesimal. Applying the following approximation

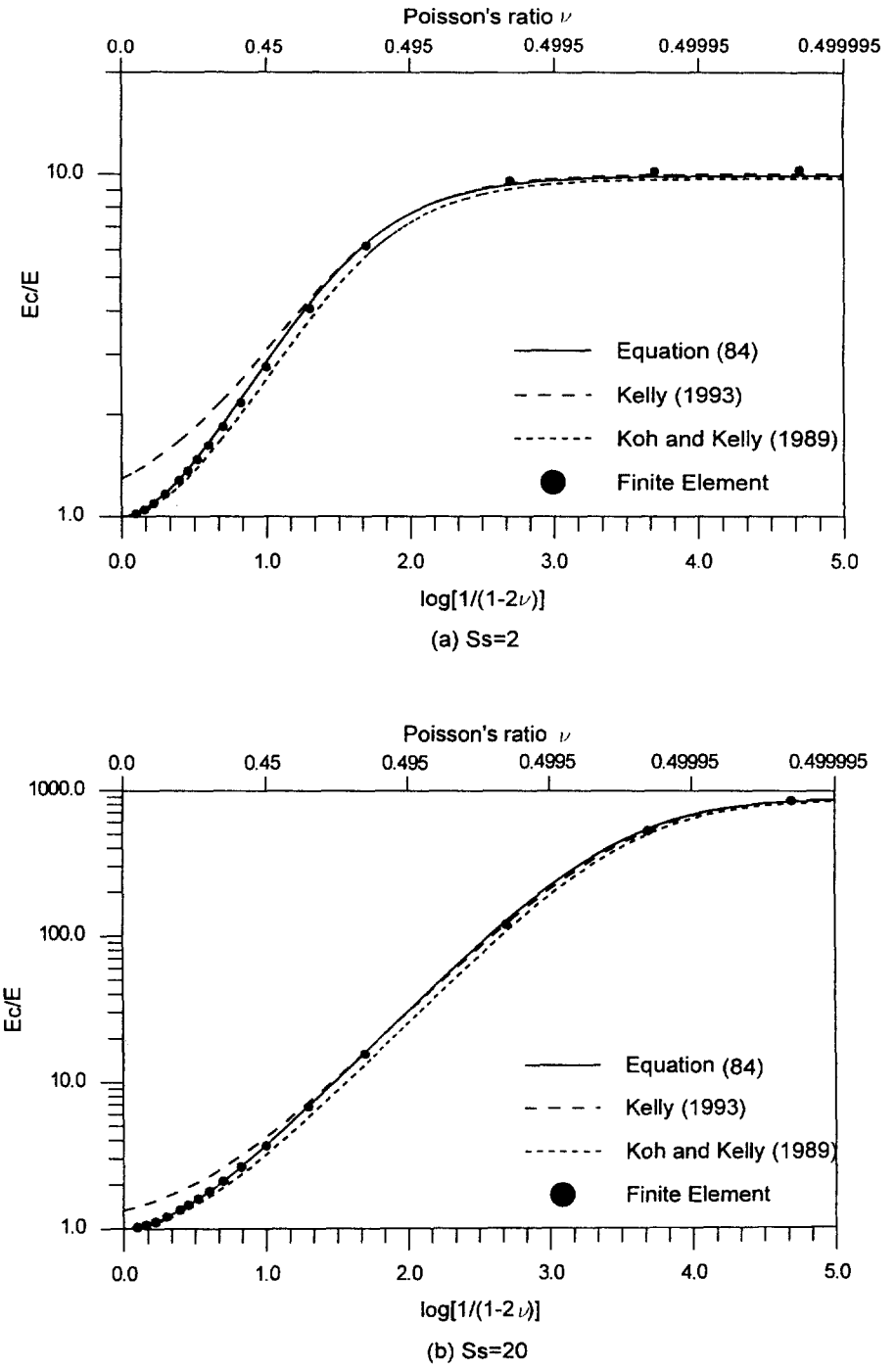

Fig. 9. Effective compression modulus of square layer.

$$\frac{\tanh(\alpha b)}{\alpha b} \approx 1 - \frac{1}{3}(\alpha b)^2 \tag{85}$$

in eqn (84), the effective compression modulus for incompressible material is found

$$E_c^{(1)} = 3\mu(1 + 2.232S^2) \tag{86}$$

If the fifty terms of a_n are considered in eqn (71), the effective compression modulus for incompressible material becomes

$$E_c^{(50)} = 3\mu(1+2.249S^2) \tag{87}$$

which is extremely close to the results published previously (Gent and Meinecke, 1970; Kelly, 1993).

6. CONCLUSION

Based on the two kinematics assumptions, i.e. horizontal planes remain plane and vertical lines become parabolic after deformation, the closed-form solutions to the compressive stiffness of elastic layers bonded between rigid plates are derived through theoretical approach for the layers of infinite-strip, circular and square shapes. The compressive stiffnesses calculated by the derived formulae are rather close to the solutions of the finite element analysis for a variety of shape factors and Poisson's ratios. This finding suggests that the two kinematics assumptions are realistic.

For the layers of infinite-strip and circular shapes, the compressive stiffnesses calculated by the derived formulae are the same as the values of Lindley (1979), although the formulae have different forms, revealing that the assumption on volume strain made by Lindley (1979) is exact, but unnecessary.

The major difference between the approach proposed herein and the method of the "approximate pressure" solution is that the latter method assumed the normal stress components to be approximated by the mean pressure. Without any stress assumption in the present approach, the governing equations of mean pressure are derived from the exact equilibrium equations and the solution of mean pressure are solved by satisfying the exact boundary conditions. The compressive stiffness solved by the present approach is very close to the "approximate pressure" solution when Poisson's ratio is greater than 0.45, but becomes smaller than the "approximate pressure" solution for lower Poisson's ratios.

Acknowledgements—The authors would like to thank the National Science Council, Republic of China, for supporting the research work reported in this paper under Grant No. NSC 85-2211-E011-014.

REFERENCES

Chalhoub, M. S. and Kelly, J. M. (1990) Effect of bulk compressibility on the stiffness of cylindrical base isolation bearings. *International Journal of Solids and Structures* **26,** 734–760.

Chalhoub, M. S. and Kelly, J. M. (1991) Analysis of infinite-strip-shaped base isolator with elastomer bulk compression. *Journal of Engineering Mechanics, ASCE* **117,** 1791–1805.

Gent, A. N. and Lindley, P. B. (1959) The compression of bonded rubber blocks. *Proceeding of the Institution Mechanical Engineers* **173,** 111–117.

Gent, A. N. and Meinecke, E. A. (1970) Compression, bending and shear of bonded rubber blocks. *Polymer Engineering and Science* **10,** 48–53.

Kelly, J. M. (1993) *Earthquake-Resistant Design with Rubber*. Springer-Verlag, London.

Koh, C. G. and Kelly, J. M. (1989) Compression stiffness of bonded square layers of nearly incompressible material. *Engineering Structures* **11,** 9–15.

Lindley, P. B. (1979) Compression module for blocks of soft elastic material bonded to rigid end plates. *Journal of Strain Analysis* **14,** 11–16.